Journal of
Synchrotron Radiation

ISSN 0909-0495

Received 14 February 2013
Accepted 3 July 2013

Combined measurement of X-ray photon correlation spectroscopy and diffracted X-ray tracking using pink beam X-rays

Yuya Shinohara,[a,b]* Akira Watanabe,[a] Hiroyuki Kishimoto[c,a] and Yoshiyuki Amemiya[a,b]

[a]Department of Advanced Materials Science, Graduate School of Frontier Sciences, The University of Tokyo, 5-1-5 Kashiwanoha, Kashiwa, Chiba 277-8561, Japan, [b]JST-CREST, Japan, and [c]Material Research and Development HQS, Sumitomo Rubber Industries Ltd, 1-1-2 Tsutsuicho, Chuo, Kobe, Hyogo 651-0071, Japan. E-mail: yuya@k.u-tokyo.ac.jp

Combined X-ray photon correlation spectroscopy (XPCS) and diffracted X-ray tracking (DXT) measurements of carbon-black nanocrystals embedded in styrene–butadiene rubber were performed. From the intensity fluctuation of speckle patterns in a small-angle scattering region (XPCS), dynamical information relating to the translational motion can be obtained, and the rotational motion is observed through the changes in the positions of DXT diffraction spots. Graphitized carbon-black nanocrystals in unvulcanized styrene–butadiene rubber showed an apparent discrepancy between their translational and rotational motions; this result seems to support a stress-relaxation model for the origin of super-diffusive particle motion that is widely observed in nanocolloidal systems. Combined measurements using these two techniques will give new insights into nanoscopic dynamics, and will be useful as a microrheology technique.

Keywords: X-ray photon correlation spectroscopy; diffracted X-ray tracking; dynamics; coherent X-rays; microrheology.

1. Introduction

Observation of the nanoscopic motion of particles enables determination of the local viscoelastic properties of a medium. This is called microrheology, and has been widely used for various materials (MacKintosh & Schmidt, 1999; Waigh, 2005). Among various microrheology techniques, light scattering is used to determine viscosity *via* the Stokes–Einstein relationship, or to reveal local viscoelastic properties using a generalized Stokes–Einstein relationship (Waigh, 2005).

Recent developments in X-ray photon correlation spectroscopy (XPCS) have enabled us to extend scattering-based microrheology into the X-ray region (Waigh, 2005; Cicuta & Donald, 2007; Leheny, 2012). XPCS is a method of observing nanoscopic dynamics based on fluctuations in the X-ray speckle scattering intensity (Sutton, 2008; Leheny, 2012). By applying X-rays to a microrheology probe, tiny motions can be observed and opaque specimens can be investigated. Recently, the application of XPCS as a microrheological technique has become popular. For example, the local viscosity inside a thin layer has been clarified using nanoparticles as markers (Koga *et al.*, 2010, 2011). In most cases, the q-range of XPCS is limited to a small-angle region and covers a scale larger than nanoparticle size; the observed dynamics therefore corresponds to diffusion of particles and/or changes in configurations and not to the rotation or deformation of particles. Even when the q-range is high enough to cover rotational motion of particles, it is difficult to distinguish between the rotational motion and the translational motion without *a priori* knowledge. Moreover, coherent X-ray intensity in such a q-range is usually not high enough to acquire quantitative data. Measurements of rotational motions using other methods in addition to translational motion will provide useful information on the nature of microscopic local viscoelastic properties.

Such observations of the rotational motion of nanoparticles can be achieved using diffracted X-ray tracking (DXT). DXT has been developed as a novel technique for investigating very small rotational motions of nanocrystals (Sasaki *et al.*, 2000, 2001). In DXT, the movements of diffraction spots from single nanocrystals are tracked. The movement directly reflects the rotational motion of the nanocrystals, not the averaged one. DXT has been applied to various systems; an important example was observation of the twisting motion of a single ion channel upon gating by attaching gold nanocrystals to the channel (Shimizu *et al.*, 2008).

A combination of XPCS and DXT reveals the detailed motion of nanocrystals in a medium. Experimentally, XPCS requires a monochromatic beam because the longitudinal coherence length should be longer than the path difference, whereas DXT requires a wide energy range to increase the probability of diffraction spots being on the Ewald sphere shells, that is, the movement of the diffraction is monitored. This experimental incompatibility can be overcome by using a 'pink' beam. Using the helical undulator at BL40XU, SPring-8

(Inoue *et al.*, 2001), moderately monochromated X-rays can be obtained without installing monochromators. In this short communication, we demonstrate combined XPCS and DXT measurements using a pink beam, and describe the potential of this technique.

2. Materials and methods

Combined XPCS and DXT measurements were performed at BL40XU, SPring-8 (Inoue *et al.*, 2001). A schematic diagram of the experimental set-up is shown in Fig. 1(*a*). A partially coherent X-ray pink beam was produced by inserting a pinhole of diameter 5 µm into quasi-monochromatic X-rays from a helical undulator. The spectrum of X-rays, measured with a Si (111) monochromator, is shown in Fig. 1(*b*). The undulator gap was 11.4 mm and the peak energy was 10.81 keV. $\Delta E/E$ was 2.7% at the half maximum and 8.1% at 1/10 of the maximum. This rather wide band restricts the q-range in which coherent scattering is observed: the longitudinal coherence length is roughly estimated to be $l = (E/\Delta E)\lambda = 4.25$ nm, where λ is the X-ray wavelength. The q-range that satisfies the condition that the path difference be shorter than the longitudinal coherence length is $q < 4.66 \times 10^{-2}$ nm^{-1} for a beam size of 5 µm; here, q is defined by $q = (4\pi/\lambda)\sin\theta$, where 2θ is the scattering angle. Speckle patterns at a small-angle region were recorded using an indirectly illuminated X-ray image intensifier coupled with an interline-CCD detector (C4880-80, Hamamatsu Photonics Ltd, Japan) (Shinohara *et al.*, 2010*a*). The distance between the sample and the detector was approximately 3 m. The speckle patterns were successively recorded with an exposure time of 436 ms. Diffraction spots from nanocrystals were observed using a CMOS flat-panel detector (C9728DK, Hamamatsu Photonics Ltd, Japan) (Yagi & Inoue, 2007). This CMOS detector was placed just downstream of the sample to track the q-range of the diffraction spots, as described below. The diffraction patterns were recorded successively with an exposure time of 2 s. The incident X-ray intensity was 3×10^{10} photon s^{-1}.

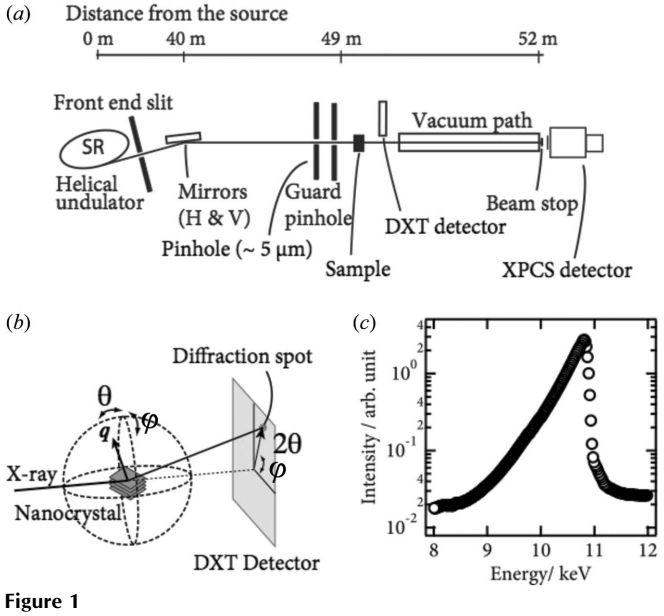

Figure 1
(*a*) Schematic view of the XPCS–DXT experimental set-up. (*b*) Geometry of the DXT experiment. Motion of the nanocrystal is defined as that of the vector normal to the diffraction plane (***q***). Geometrical correlations between the movements of the vector in the real space and those of the spot on the image frame are shown. (*c*) Spectrum of incident X-rays measured with a Si (111) monochromator.

We used graphitized carbon-black nanocrystals embedded in commercial-grade unvulcanized styrene–butadiene rubber as the sample. The volume fraction of nanocrystals was 1%. Transmission electron microscopy and small-angle X-ray scattering studies showed that the averaged nanocrystal radius was approximately 1×10^2 nm, with a wide size distribution. The sample was set in a temperature-controlled stage (Linkam Scientific Instruments Ltd, THMS-600) and its temperature was kept at 423 K. The nanocrystals show two distinct interlayer diffractions at $q = 18.8$ nm^{-1} (002) and 37.5 nm^{-1} (004), and a rather broad in-plane diffraction at 30.03 nm^{-1} (10) (Warren, 1941; Biscoe & Warren, 1942); the movements of these diffraction spots were tracked using DXT. The θ-range, $\Delta\theta$, at each diffraction spot for the present experimental setting can be estimated from the differential form of Bragg's law: $\Delta\theta \simeq \tan\theta(\Delta\lambda/\lambda)$. Note that the spectrum shows a long tail in a lower X-ray energy region since a raw X-ray spectrum from the helical undulator is observed; hence 002 diffraction spots, for example, can be observed in the range $9.28^\circ < \theta < 12.6^\circ$, when the intensity of a diffraction spot is high enough. Based on the energy spectrum, the number of nanoparticles in the illuminated volume and the X-ray wavelength, the average number of diffraction spots detected in the present setting can be calculated to be ~10, which was consistent with the number of diffraction spots observed experimentally.

3. Results and discussion

3.1. XPCS results

Fig. 2 (right) shows the dependence of the relaxation time τ and the exponent p on q. The time-correlation functions of scattering intensity were analyzed using a single exponential function, as in a previous study (Shinohara *et al.*, 2010*b*): $g^{(2)}(t) = 1 + A\exp[-2(t/\tau)^p]$, where p, A and τ correspond to the Kohlrausch–Williams–Watts exponent, the optical contrast and the relaxation time, respectively. The fitting results are also shown in Fig. 2 (right). The exponent p is larger than unity, which indicates super-diffusive motion of the nanocrystals. This behavior is generally observed for nanoparticles in unvulcanized rubber (Shinohara *et al.*, 2010*b*, 2012), vulcanized rubber (Ehrburger-Dolle *et al.*, 2012) and many other systems (Leheny, 2012). The dependence of τ on q shows a simple power law: $\tau \simeq q^{-0.65}$. The results show that the nanocrystal dynamics is not described by simple diffusive behavior; the origin and mechanism of the complex dynamics is beyond the scope of the present manuscript and requires further studies.

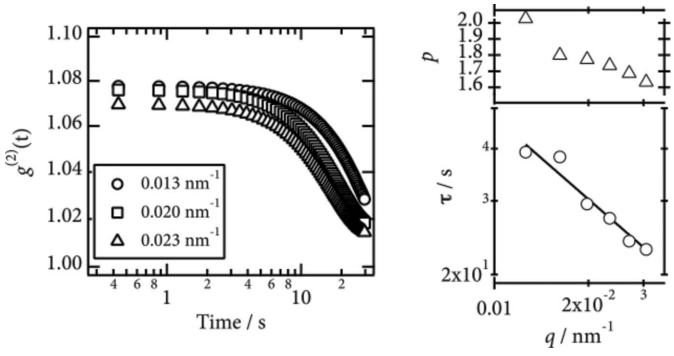

Figure 2
(Left) Typical intensity–intensity correlation function. (Right) Dependence of relaxation time τ and the exponent p on q. The line shows the fit to the data.

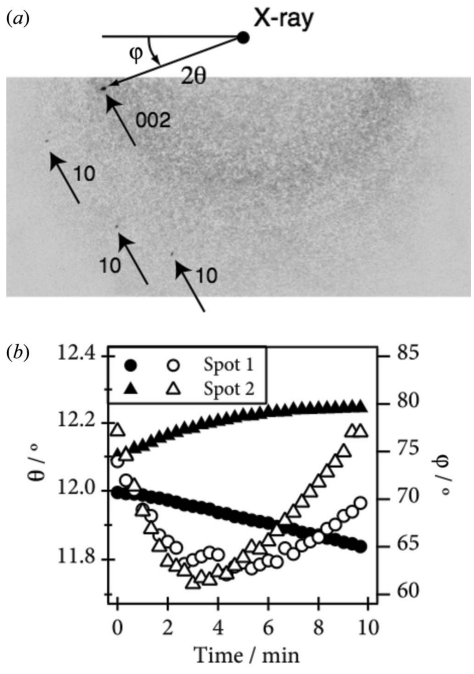

Figure 3
(*a*) Example of a diffraction image. Several diffraction spots from the (002) and (10) planes are observed. (*b*) Time-evolution of θ and φ from two 002 diffraction spots out of 37 spots. The other spots show a similar behavior. Open symbols and closed symbols correspond to θ and φ, respectively.

3.2. DXT results

A diffraction image measured using the X-ray flat-panel detector is shown in Fig. 3(*a*). Diffraction spots from (002) and (10) are clearly observed. By tracking the positions of spots, we calculated the time-evolution of φ and θ, as shown in Fig. 3(*b*). In this way, the translational and rotational motion can be simultaneously observed by combining XPCS and DXT.

3.3. Discussion and prospects

The rotational motion is extremely 'slow' compared with the dynamics observed in XPCS; the characteristic time of rotational motion is estimated to be several minutes, whereas the relaxation time observed with XPCS is a few tens of seconds. Note that the speckle pattern in the XPCS measurements originates from the nanocrystal configuration in the present case; thus, collective or mutual diffusive motion rather than self-diffusive motion is observed in the present XPCS while self-rotational motion is observed in DXT. The discrepancy between the time scales of translational and rotational motion would provide a clue to the nature of the super-diffusive nanocolloidal dynamics commonly measured with XPCS as well as the present study. There are two leading hypotheses for the origin of this motion (Madsen *et al.*, 2010): (i) strain in response to relaxation of local heterogeneous stress (Bouchaud & Pitard, 2001; Cipelletti *et al.*, 2003) and (ii) the continuous-time random walk (CTRW) model (Caronna *et al.*, 2008). In the stress-relaxation picture, advected particles would primarily undergo translational motion while maintaining almost time-independent orientations for strain fields with strain gradients that are small on the particle scale; hence this picture provides a natural explanation for the discrepancy of timescales in the XPCS and DXT measurements. In contrast, it seems difficult to interpret the results in the context of the CTRW model. Although additional theoretical work is required to determine the microscopic picture of the dynamics and to explain the behavior of p, which is larger than the calculated value of 1.5 (Bouchaud & Pitard, 2001), further investigation using this combined measurement will clarify the origin and provide useful information about the dynamics of nanocrystals in a medium.

This work provides a way to probe the rotational and translational dynamics of nanocrystals, and it can be applied to various systems. For example, the motion of nanocrystals in rubber reveals the mechanism of the reinforcement effect of rubber, whereby the viscoelastic and mechanical properties are significantly improved. Recently, XPCS has started to be used for investigating the relationship between macroscopic viscoelasticity and the microscopic motion of nanoparticles such as carbon-black and silica (Shinohara *et al.*, 2010*b*, 2012; Ehrburger-Dolle *et al.*, 2012). However, the nature of the nanoparticles dynamics has not yet been clarified. Information on the rotational motion from DXT measurements not only helps us interpret the XPCS data but also enables us to reveal the mechanism of reinforcement effects. For example, the interface between nanocrystals and a surrounding medium is important because the slip/stick condition at the interface affects the diffusive motion of the nanocrystals; the friction at the interface leads to energy loss of materials. In this regard, the use of well controlled nanocrystals as a probe is the key to elucidating the nature of dynamics; we plan to develop such nanocrystals.

To conclude, we have successfully demonstrated combined XPCS and DXT measurements; the translational and rotational motions of nanocrystals in rubbery materials were simultaneously observed. The combined measurements will give new insights into nanoscopic dynamics.

The authors thank Drs N. Ohta, K. Aoyama and N. Yagi for their experimental support. The XPCS–DXT experiment was performed under the approval of the JASRI Program Advisory Committee (Proposal Nos. 2012A1070 and 2012B1101). This study was supported by JSPS KAKENHI (No. 24710092).

References

Biscoe, J. & Warren, B. E. (1942). *J. Appl. Phys.* **13**, 364–371.
Bouchaud, J.-P. & Pitard, E. (2001). *Eur. Phys. J. E*, **6**, 231–236.
Caronna, C., Chushkin, Y., Madsen, A. & Cupane, A. (2008). *Phys. Rev. Lett.* **100**, 055702.
Cicuta, P. & Donald, A. M. (2007). *Soft Matter*, **3**, 1449.
Cipelletti, L., Ramos, L., Manley, S., Pitard, E., Weitz, D. A., Pashkovski, E. E. & Johansson, M. (2003). *Faraday Discuss.* **123**, 237–251.
Ehrburger-Dolle, F., Morfin, I., Bley, F., Livet, F., Heinrich, G., Richter, S., Piché, L. & Sutton, M. (2012). *Macromolecules*, **45**, 8691–8701.
Inoue, K., Oka, T., Suzuki, T., Yagi, N., Takeshita, K., Goto, S. & Ishikawa, T. (2001). *Nucl. Instrum. Methods Phys. Res. A*, **467**, 674–677.
Koga, T., Jiang, N., Gin, P., Endoh, M. K., Narayanan, S., Lurio, L. B. & Sinha, S. K. (2011). *Phys. Rev. Lett.* **107**, 225901.
Koga, T., Li, C., Endoh, M. K., Koo, J., Rafailovich, M., Narayanan, S., Lee, D. R., Lurio, L. B. & Sinha, S. K. (2010). *Phys. Rev. Lett.* **104**, 066101.
Leheny, R. L. (2012). *Curr. Opin. Colloid Interface Sci.* **17**, 3–12.
MacKintosh, F. C. & Schmidt, C. F. (1999). *Curr. Opin. Colloid Interface Sci.* **4**, 300–307.
Madsen, A., Leheny, R. L., Guo, H., Sprung, M. & Czakkel, O. (2010). *New J. Phys.* **12**, 055001.
Sasaki, Y. C., Okumura, Y., Adachi, S., Suda, H., Taniguchi, Y. & Yagi, N. (2001). *Phys. Rev. Lett.* **87**, 248102.
Sasaki, Y., Suzuki, Y., Yagi, N., Adachi, S., Ishibashi, M., Suda, H., Toyota, K. & Yanagihara, M. (2000). *Phys. Rev. E*, **62**, 3843–3847.

Shimizu, H., Iwamoto, M., Konno, T., Nihei, A., Sasaki, Y. C. & Oiki, S. (2008). *Cell*, **132**, 67–78.
Shinohara, Y., Imai, R., Kishimoto, H., Yagi, N. & Amemiya, Y. (2010*a*). *J. Synchrotron Rad.* **17**, 737–742.
Shinohara, Y., Kishimoto, H., Maejima, T., Nishikawa, H., Yagi, N. & Amemiya, Y. (2012). *Soft Matter*, **8**, 3457.
Shinohara, Y., Kishimoto, H., Yagi, N. & Amemiya, Y. (2010*b*). *Macromolecules*, **43**, 9480–9487.
Sutton, M. (2008). *C. R. Phys.* **9**, 657–667.
Waigh, T. A. (2005). *Rep. Prog. Phys.* **68**, 685–742.
Warren, B. E. (1941). *Phys. Rev.* **59**, 693–698.
Yagi, N. & Inoue, K. (2007). *J. Appl. Cryst.* **40**, s439–s441.